Available online at www.sciencedirect.com
SCIENCE DIRECT®
Solid State Ionics 165 (2003) 191–200
SOLID STATE IONICS
www.elsevier.com/locate/ssi

Preparation and structural investigations of electrochromic nanosized NiO_x films made via the sol–gel route

R. Cerc Korošec[a], P. Bukovec[a,*], B. Pihlar[a], A. Šurca Vuk[b], B. Orel[b], G. Dražič[c]

[a] Faculty of Chemistry and Chemical Technology, Aškerčeva 5, SI-1000 Ljubljana, Slovenia
[b] National Institute of Chemistry, Hajdrihova 19, SI-1001 Ljubljana, Slovenia
[c] Jožef Stefan Institute, Jamova 39, SI-1001 Ljubljana, Slovenia

Abstract

The main aim of this work was to study the influence of the $NiSO_4$ precursor and the annealing temperature on the electrochemical stability and electrochromic response of dip-coated Ni-oxide films. Nickel hydroxide was precipitated from the precursor solution using lithium hydroxide and the slurry was then peptized with acetic acid. Dynamic thermogravimetric measurements made on thin films showed that the decomposition and the formation of Ni-oxide phase differed for powders and films. The results showed that the films annealed at 270 °C (at which the acetate groups decomposed) consisted of cubic (space group Fm3m) NiO grains (2–3 nm, TEM measurements) having monodentately coordinated sulfate groups (IR spectrum). Electrochemical and in situ UV–visible spectroelectrochemical studies of the Ni-oxide films ($NiSO_4$ precursor, 270 °C) revealed that the photopic transmittance in the colored state (3rd cycle) is 66% and 89% in the bleached state. Cycling (100th cycle) reduced the transmittance of the films in the colored state to 50%, while the bleached films retained their high transmittance (89%). The coloration efficiency of the films was 35–41 $cm^2\ C^{-1}$ depending on the number of cycles. The evolution of the Ni^{3+}–O stretching vibration (transversal optical mode) of the films in the charged state was followed by the help of ex situ infrared spectroelectrochemical measurements.

PACS: 78.20.Jq; 81.20.Fw
Keywords: Electrochromism; NiO thin films; Thermogravimetry; Optimisation; Sol–gel; IR spectroscopy; TO modes

1. Introduction

Nickel oxide thin films have been widely studied for application as an optically active layer in electrochromic devices [1]. Under anodic potentials they change color from transparent to deep brown [2]. They exhibit a high coloration efficiency, neutral coloration and stability in basic (protic) electrolytes [2,3]. Among various deposition techniques the sol–gel process combined with dip-coating deposition is important because the final properties of the films can be tailored using various precursors and different annealing temperatures [4].

It is well known for these films that a degree of thermal treatment is the key factor which determines the electrochromic effect during potential cycling. Too high a processing temperature significantly lowers the

* Corresponding author. Tel.: +386-1-2419-128; fax: +386-1-2419-143.
E-mail address: peter.bukovec@uni-lj.si (P. Bukovec).

0167-2738/$ - see front matter © 2003 Elsevier B.V. All rights reserved.
doi:10.1016/j.ssi.2003.08.032

electrochromic effect [5–8], and the layer could even become inactive [7,9,10]. On the other hand, in thermally untreated films either the optical modulation decreases soon after the beginning of cycling [11,12], or the film becomes detached from the substrate [13,14].

When the sample is prepared as a thin film or in powdered form, the differences in the particle size and in the microstructure of the two forms lead to different thermal stabilities. It is well known that the decomposition temperature decreases with decrease in sample particle size [15]. Therefore, it is extremely important to perform thermal analysis on the thin films themselves rather than on the corresponding xerogels.

Thermal analysis of thin films is a demanding procedure and direct measurements of thin films are still not very common [16]. This is the reason why in most articles which report thin film properties thermal analysis is either made on the corresponding xerogels [3,9,17–19] or the investigated films are thermally treated at 250 or 300 °C without performing TG analysis even for the xerogels [8,20]. The sensitivity of balances in TG instruments is in the order of 1 μg so that detection of the thermal decomposition of the thin film is possible [21]. But the amount of sample available is small, typically below 1 mg cm^{-2}, so that the mass change during a TG experiment is in the range of buoyancy and aerodynamic effects. In order to overcome these problems, large area samples were used [22–24] or the measurements carefully performed—for instance with subtraction of the blank curve [25] or by high resolution TG [26].

The aim of our work was to study the evolution of thin film structure during heat treatment using FTIR and TEM analysis. From the results of dynamic TG curves of thin films the processing temperature at which the formation of nickel oxide takes place can be chosen. Knowing the shape of the isothermal TG curve, several thin films with different ratios between the thermally undecomposed amorphous phase and nanosized nickel oxide could be prepared by regulating the duration of heat treatment at isothermal temperature. The electrochromic stability of these films was tested by in situ UV–VIS spectroelectrochemical measurements during cycling in 0.1 M LiOH up to 100 cycles. The photopic transmittance values [27] of thermally untreated film was compared to the values obtained for optimised films.

2. Experimental

2.1. Preparation of sol and xerogel

LiOH (2.0 M; Kemika, Zagreb, Croatia) was added dropwise with stirring to a 0.5 M solution of nickel sulfate (Kemika) until pH 9.0 was reached. The green precipitate was washed several times with water. The slurry was then peptized with glacial acetic acid to pH 4.5. Some water was added to obtain an appropriate viscosity. The sol was then sonicated and filtered. To obtain corresponding xerogel the sol was poured into petri dishes and left to dry.

2.2. Instrumental

2.2.1. TG measurements

For TG measurements, thin films were deposited on microscope slide glasses. Before deposition a wetting agent (a solution of 1 wt.% of Etolat TD-60; TEOL Factory, Ljubljana, Slovenia; in distilled water) was dispersed on the substrate. After the wetting solution had dried, the thin film was deposited with a pulling velocity of 5 cm min^{-1}. Thermoanalytical measurements were performed on a Mettler Toledo TGA/SDTA 851^e instrument. In dynamic measurements, the temperature range from room temperature up to 900 °C was applied for the xerogel and from 25 to 600 °C for thin films deposited on glass substrates. The initial mass of the xerogel was approximately 10 mg and of the thin film sample (thin film + substrate) around 100 mg. Microscope-cover glasses with deposited films were placed between two clean sheets of paper and then broken into small pieces suitable for placing in the pan. Platinum crucibles (diameter 8 mm) and a heating rate of 5° min^{-1} were used in dynamic measurements. In isothermal measurements, the furnace was heated at 2° min^{-1} to the chosen temperature, left at that temperature for 90 min and then heated up to 350 °C at 2° min^{-1}. The baseline was subtracted in all cases.

2.2.2. IR measurements

Fourier transform infrared (FT-IR) spectroscopic measurements were made using a Perkin Elmer System 2000 Spectrophotometer with a resolution of 4 cm^{-1}. To obtain transversal optical (TO) modes, the films were deposited on Si wafers. Before thin film

deposition, a wetting agent (1 wt.% of Etolat in distilled water) was deposited on the substrate.

2.2.3. Spectroelectrochemical measurements

In situ chronocoulometric measurements were performed using a Perkin Elmer UV/VIS Lambda 2 Spectrometer, connected to an EG and G PAR Model 273 computer-controlled potentiostat–galvanostat. A homemade three-electrode spectroelectrochemical transmission cell, filled with 40 ml of 0.1 M LiOH was used. A Pt rod served as the counter electrode, an $Ag/AgCl/KCl_{sat}$ cell as the reference electrode ($E=0.197$ V) and a thin Ni-oxide film deposited on SnO_2/F glass (square resistivity 13 Ω/□) as the working electrode (area 1×3.5 cm). For background measurements, a cell filled with only the electrolyte was used. In situ UV–VIS spectroelectrochemical measurements were made in the range 360–1100 nm under the same conditions.

The weighted photopic transmittance (T_{vis}) was calculated from the formula:

$$T_{vis} = \frac{\sum_{380nm}^{780nm} D_\lambda \tau(\lambda) V(\lambda) \Delta\lambda}{\sum_{380nm}^{780nm} D_\lambda V(\lambda) \Delta\lambda}$$

where λ represents the wavelength of light, $\tau(\lambda)$ the spectral transmittance of the sample, D_λ the spectral energy distribution of the solar radiation and $V(\lambda)$ the luminous efficiency of the human eye. Zero reflectance was used in the calculation as an approximation.

2.2.4. TEM study

Plan-view specimens of thin film samples were prepared by mechanical thinning, dimpling and ion milling from the substrate side. A cross section of the sample on a ⟨Si⟩ substrate was prepared using a Gatan cross-sectional TEM specimen preparation kit. After mechanical thinning and dimpling, ion milling using 3.8 keV argon ions at 10° incident angle was used. To prevent degradation, the samples were cooled with liquid nitrogen during the final stages of the ion erosion process. Samples were examined by a JEOL 2000 FX transmission electron microscope, operated at 200 kV. The chemical composition of the phases was determined using a Link AN-1000 energy dispersive X-ray spectroscopy (EDXS) system with an ultra-thin window Si(Li) detector.

3. Results and discussion

Dynamic thermogravimetric measurements of a thin film and the corresponding xerogel powder under an air atmosphere are presented in Fig. 1. Two phenomena can be observed in the dynamic TG curve of the thin film. Firstly, the curve is not smooth because the very small mass loss (~ 0.1% in the whole temperature range) means that the digital noise of the instrument is appreciable. Secondly, in the temperature range from approximately 100 to 200 °C a slight increase in the weight is observed. Although the baseline (TG curve of empty pan) was subtracted, small variations in the flow rate of the purging gas may have caused a weight gain.

From room temperature up to 200 °C dehydration takes place [4]. The onset decomposition temperature of acetate groups is 280 °C for the thin film sample and 300 °C for the xerogel (insert in Fig. 1). During thermal decomposition of acetates (see the evolution of the IR spectra in Fig. 2) nano-grains of nickel oxide are formed (TEM micrograph, Fig. 3a). The third step in the TG curve of the xerogel around 700 °C is attributed to thermal decomposition of the sulfate groups, which remain coordinated to nickel cations during the preparation of the sol. For the thin film, the dynamic TG measurement was performed only to 600 °C; above this temperature microscope cover glasses begin to soften.

Isothermal TG curves of both forms of the sample at 270 and 300 °C are shown in Fig. 4a, b. The temperature was chosen on the basis of the dynamic measurements of the thin film and the xerogel (Fig. 1). After isothermal treatment, the temperature in the furnace was increased to 350 °C where decomposition is complete for both types of samples. From the ratio of the isothermal weight loss after a defined time and the weight loss associated with decomposition of all acetate groups, the degree of thermal decomposition of acetates can be estimated. For the thin film, the degree of the thermal decomposition is 50% after 15 min, 80% after 30 min and 100% after 60 min (Fig. 4a). Only 30% decomposition of the xerogel was observed at 270 °C after 60 min (Fig. 4b). From

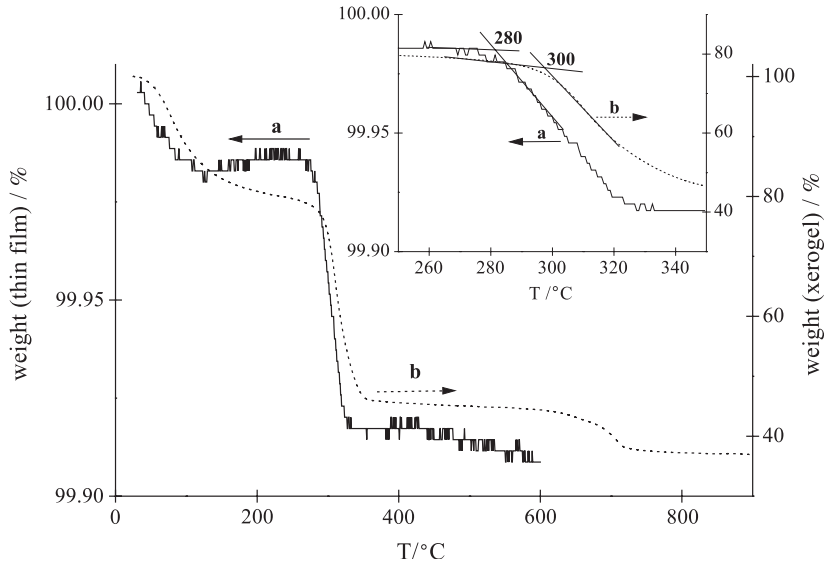

Fig. 1. Dynamic thermogravimetric curves of a thin film deposited on a microscope-cover glass (a)—left ordinate—and of the xerogel (b)—right ordinate—in a dynamic air atmosphere.

analogous measurements at 300 °C, we noted that the thermal decomposition of the xerogel is completed after 85 min, while for the thin film this occurs after 12 min. Thin films with different ratios between thermally undecomposed amorphous phase and nickel oxide can be prepared by controlling the time of heat treatment at 270 °C. At 300 °C, the decomposition process is much faster.

In the IR spectrum of a thermally untreated film (Fig. 2a), the bands at 1565 and 1419 cm^{-1} belong to asymmetric ($\nu_a(COO^-)$) and symmetric ($\nu_s(COO^-)$) vibrations of the acetate groups [28]. $\nu_a(COO^-)$ and $\nu_s(COO^-)$ for free acetate ions are at 1556 and 1413 cm^{-1}, their difference being 144 cm^{-1}. On the basis of this difference ($\Delta\nu$) one can deduce the type of coordination of the acetate groups to the metal ions [28]. Regarding the free ion, $\Delta\nu$ in the bridging complex remains practically unchanged. We can therefore suppose that in the thermally untreated xerogel the acetate groups are mostly present as bridging ligands to nickel ions. The peaks at 1345, 1053 and 1029 cm^{-1} reveal the presence of methyl groups ($\delta(CH_3)$). The band at 1111 cm^{-1} belongs to a stretching vibration of the free sulfate groups with T_d symmetry, and the shoulder around 1175 cm^{-1} to the bridging sulfate groups with C_{2v} symmetry [29]. Comparison of the two intensities shows that some SO_4^{2-} groups remain free in the structure. The bending vibration of the free sulfate anion is at 613 cm^{-1} and that of a bridging one at 641, 610 and 571 cm^{-1}. All peaks except that at 571 cm^{-1} are of strong intensity. In the thermally untreated sample the out-of-plane vibration of acetate groups is superimposed on the bending vibration of the sulfate groups, and therefore the latter are not clearly expressed. The band at 678 cm^{-1} is attributed to the δ(OCO) vibration and that at 616 cm^{-1} to π(COO), π(CH) as well as SO_4^{2-} bending vibrations.

The IR spectrum of the thin film after dehydration (15 min at 220 °C, Fig. 2b) is similar to that of the thermally untreated film. The shoulder at 1185 cm^{-1} becomes more pronounced. This means that during dehydration more sulfate groups bind to nickel, otherwise the thin film structure remains practically unchanged.

The bands associated with the acetate motions become smaller in the IR spectrum of the thin film thermally treated at 270 °C for 15 min (Fig. 2c). The vibrations at 1121 and 1049 cm^{-1} are attributed to stretching vibrations of the monodentately coordinated sulfate groups and those at 632 and 601 cm^{-1} to the bending vibrations of the same groups. The band that appears below 500 cm^{-1} corresponds to a stretching vibration of the Ni—O bond of nickel oxide

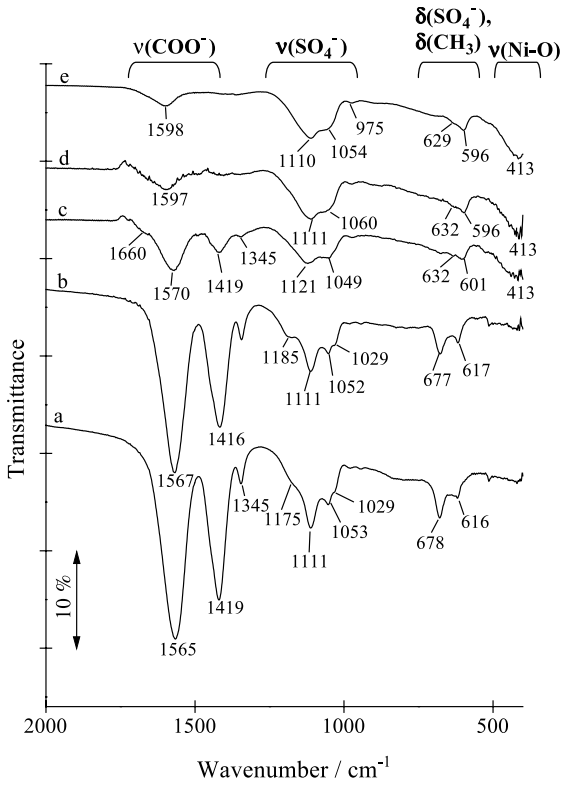

Fig. 2. IR transmittance spectra of the as deposited film (a), film thermally treated at 220 °C for 15 min (b), at 270 °C for 15 min (c), at 270 °C for 30 min (d) and at 270 °C for 60 min (e).

[30]. The shoulder around 1660 cm^{-1} can be ascribed to the C=O groups bonded on organic ($-CH_2$, $-CH_3$) groups and monodentately coordinated to nickel [28]. The appearance of the carbonyl vibration reveals the reorganization of atoms and bonds during thermal decomposition of the acetate groups.

With increasing time of heat treatment at 270 °C the vibrations of the sulfate groups as well as the Ni–O stretching band become more intense (Figs. 2d,e). The sulfate groups remain monodentately bonded to nickel ($\nu_3 = \sim 1110$, 1060 cm^{-1}, $\nu_1 = 970$ cm^{-1}, $\nu_4 = \sim 630$ and 595 cm^{-1}). The band at ~ 1600 cm^{-1} is attributed to the bending vibration of water due to absorbed moisture. A thin film thermally treated at 270 °C for 60 min consists of nano-crystals of cubic NiO with a size of 2–3 nm, as shown in the TEM micrograph (Fig. 3a). The IR spectrum of the film thermally treated at 500 °C for 15 min reveals no difference with regard to the last described spectrum.

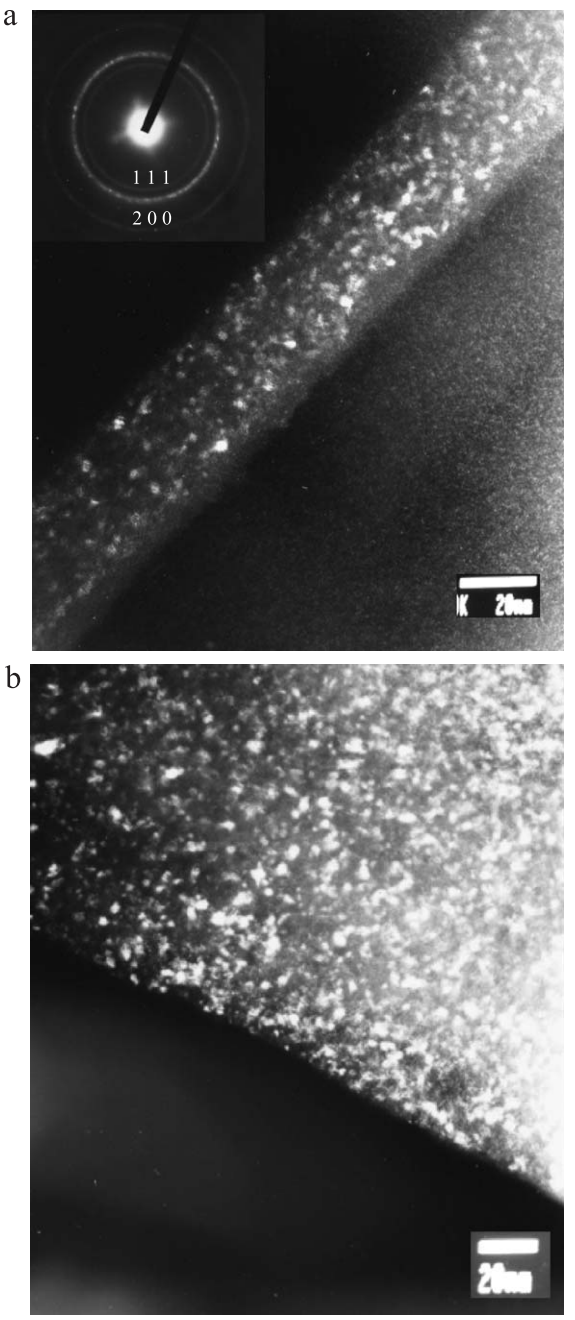

Fig. 3. Dark field image and SAED pattern (inset, indexed as cubic NiO) of the cross section of a thin film thermally treated at 270 °C for 60 min (a) and in plan-view of a thin film thermally treated at 500 °C for 15 min (b). From (a) the film thickness was estimated to be around 35 nm.

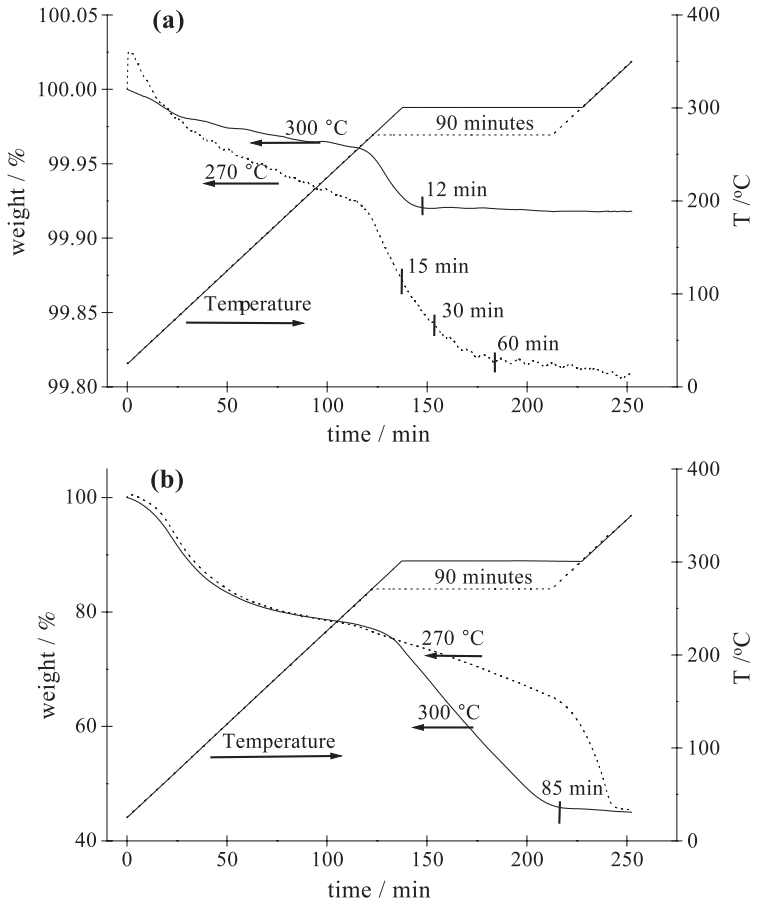

Fig. 4. Isothermal TG curves of a thin film (a) and the corresponding xerogel (b) at 270 and 300 °C.

From the TEM micrograph (Fig. 3b) it is clear that the grains of cubic NiO have grown to around 5 nm.

In situ monochromatic optical transmittance changes ($\lambda = 480$ nm) during chronocoulometric measurements of thin films thermally treated at various temperatures are shown in Fig. 5. The curves represent the responses of the stabilised 101st cycles during charging at a potential of 0.6 V vs. Ag/AgCl (0–30 s) and discharging at 0.0 V vs. Ag/AgCl (30–60 s). Thin films heated at 270 °C for 15 or 30 min (Fig. 5a,b) do not bleach to the initial value under cathodic potential, but show a higher degree of coloration under an anodic potential than films thermally treated for a longer time or at higher temperatures. Reversibility in the bleaching process is achieved for films in which thermal decomposition of the acetate groups is complete; i.e. a film thermally treated at 270 °C for 60 min, 15 min at 400 °C or 15 min at 500 °C (Fig. 5c–e). Among them the highest coloration effect is exhibited by the thin film exposed for 60 min to 270 °C. The required time to reach the maximum coloration at 0.6 V increases with increasing content of nickel oxide in the structure (Fig. 5a–c). The thicknesses of all films are 35 nm, except the one treated for 15 min at 500 °C (< 20 nm). This is one of the reasons why the latter (Fig. 5e) shows a very poor coloration effect (the number of color active centres is proportional to the film thickness) and a very quick response. Intercalation of the hydroxide ions occurs faster in the whole volume in a thinner film. Another reason for the poor coloration effect is due to the size of the nano-grains. In the film prepared at 500 °C, this is approximately twice as large (5 nm—Fig. 3b) than in the film thermally treated at 270 °C for 60 min (2.5 nm, Fig. 3a), and therefore the

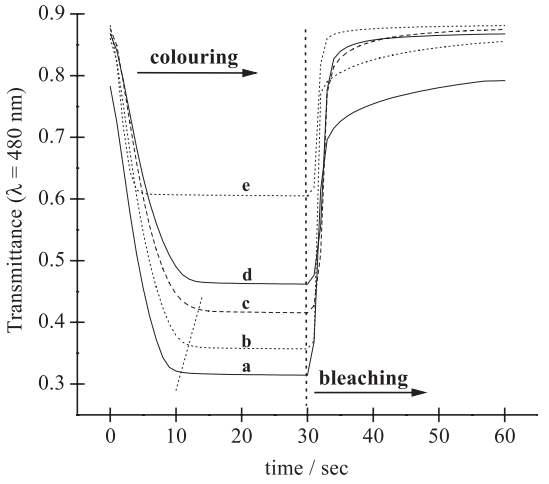

Fig. 5. In situ monochromatic transmittance changes ($\lambda = 480$ nm) during chronocoulometric measurements of a thin film thermally treated at 270 °C for 15 min (a), at 270 °C for 30 min (b), at 270 °C for 60 min (c), at 400 °C for 15 min (d) and at 500 °C for 15 min (e). The films were colored at 0.6 V for 30 s and bleached at 0.0 V for 30 s.

specific surface in the latter is larger. Assuming that electrochemical reaction takes place on the surface of the nano-grains, the coloration effect should be more pronounced in films with a larger specific surface value.

A diagram of a weighted photopic transmittance changes for the bleached and the colored state (3rd, 12th, 102nd cycle) of thin films thermally treated to the different extent is shown in Fig. 6. Optical modulation of thermally untreated film was large at the beginning of the cycling process, the difference in photopic transmittance between the colored and the bleached state for 40 nm thick film was 50%. The bleaching process of the amorphous phase was not reversible at the beginning of cycling. The transmittance at the cathodic potential was reduced for ~ 10% in the first 10 cycles. After dehydration (thin film thermally treated at 220 °C for 15 min) the optical modulation during cycling process decreased as compared to the thermally untreated film, but the bleaching process became more reversible. The calculated photopic transmittance change in 102nd cycle of this film shows that reversibility was still not achieved. The reversibility of bleaching/coloring process improves with increasing amount of NiO phase. Diminishing of amorphous phase in the structure (films kept at 270 °C for 15, 30 or 60 min) caused that optical modulation changes were smaller at the

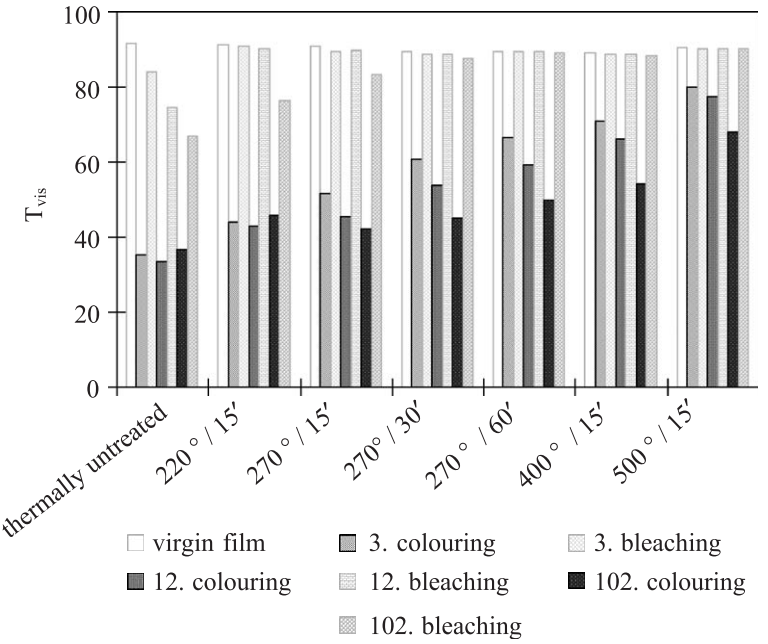

Fig. 6. Weighted photopic transmittance calculated for the 3rd, 12th and 102nd cycle of thin films thermally treated at various temperatures.

beginning of the cycling, but the reversibility was significantly improved. The photopic transmittance values at the cathodic potential of 102nd cycle showed that films, which were heat-treated 15 or 30 min at 270 °C, were still not stable. For the latter films the diminishing of photopic transmittance value for 7% (15 min at 270 °C) and 2% was observed with respect to the virgin film. The reversibility during the cycling process was obtained for the films, which were thermally treated at 270 °C for 60 min., which we related to the complete thermal decomposition of acetate groups. The electrochromic stability of these films seemed to be connected with the presence of the NiO nano-grains as shown from TEM micrographs. The presence of amorphous phase could not be excluded; however, its portion did not exceed 10%. The sulfate groups remained monodentately coordinated to nickel cations, situated either on the surface of nano-grains or in amorphous phase in between the grains. Photopic transmittance in the 3rd cycle is 66% for the colored and 89% for the bleached state. During the cycling process the transmittance in the colored state was decreased. In 12th cycle reaches 59% and in 102nd 50%, and it turns to the initial value at the cathodic potential (89%). Thin film which was kept at 400 °C for 15 min possessed similar properties as the described above; only the photopic transmittance values at the anodic potential are approximately 5% lower regardless to the number of the cycle. The reason for such behaviour could be the larger size of the grains.

Ex situ infrared transmittance spectra of virgin, soaked and charged/discharged ($Q_{ins} = Q_{ex} = 20$ mC cm^2) Ni-oxide films are represented in Fig. 7. The spectrum of the virgin film (Fig. 7a) exhibited strong OH stretching mode (3500–3000 cm^{-1}) but δ(OH) was not seen because it became blurred due to the strong bands at 1575 and 1417 cm^{-1} attributed to the vibrations of the acetate ligands. The 672 cm^{-1} band which appeared as a shoulder band also belonged to the vibrations of the acetate groups and became removed from the film after soaking in LiOH (Fig. 7b). The acetate groups became substituted with the CO_3^{2-} groups which we conceived from the presence of strong bands at 1465 and 1376 cm^{-1} (Fig. 7b) and the 1019 cm^{-1} band which is characteristic for the carbonate groups chelated to the metal ions [31]. Soaking the film in LiOH also removed the SO_4^{2-} groups. The bands at 1110 and 1063 cm^{-1} disappeared from the IR spectra showing that SO_4^{2-} groups were completely removed from the film.

The band at 617 cm^{-1} (Fig. 7a) gave the information about the Ni–O modes. More modes contributed to the absorption in this range: Ni–OH stretching at 520 cm^{-1} [30], wagging of the H_2O ($\sim$ 600 cm^{-1}) and the deformational modes of SO_4^{2-} groups (611 cm^{-1}) [29]. When the film was soaked in LiOH, the SO_4^{2-} deformational mode disappeared and as the result of that the band shifted from 617 to 632 cm^{-1} (Fig. 7b). Small shoulder band at $\sim$ 600 cm^{-1} with a tail extending to the lower frequencies signalled the presence of the Ni–OH "hydroxyl stretching" lattice mode [30] found in the range $<$600 cm^{-1} but the Ni–O stretching band found by others [30,32] in the range $<$450 cm^{-1} was not observed in the spectrum of soaked film.

However, the latter band appeared in the spectrum of colored Ni-oxide film (Fig. 7c) at 445 cm^{-1} and was accompanied with a strong and quite sharp band at 573 cm^{-1}. The assignment of both bands is unquestionable because they appeared quite close to the position of the corresponding bands observed in the spectra of NiOOH powders [30]. The difference in frequencies observed in IR spectra of thin films and powders was expected because the polarisation effects shift the mode frequencies of powders. That agreed with the nanocrystalline nature of our films exhibiting grains with dimensions 5–10 nm. The other bands (1635, 1458 and 1369 cm^{-1}) remained unchanged when the film was colored and will not be discussed further. It should be noted that the appearance of the NiO stretching band at 445 cm^{-1} indicated the evolution of the NiO phase embedded in the NiOOH phase when the film was colored.

In the spectra of bleached film (Fig. 7d), the 573 cm^{-1} band shifted to 591 cm^{-1} while the NiO stretch at 445 cm^{-1} remained unaffected. The 573 cm^{-1} band became much broader suggesting that the local structure around Ni atoms changed; strongly bonded OH group to Ni central atom in the NiOOH phase became relaxed and the Ni–O stretching shifted to higher frequencies as the consequence of the reduced effective mass of the OH groups which surrounded the Ni atoms. The process was reversible for a few following cycles. The differences in the spectra between the colored and bleached state (not shown here)

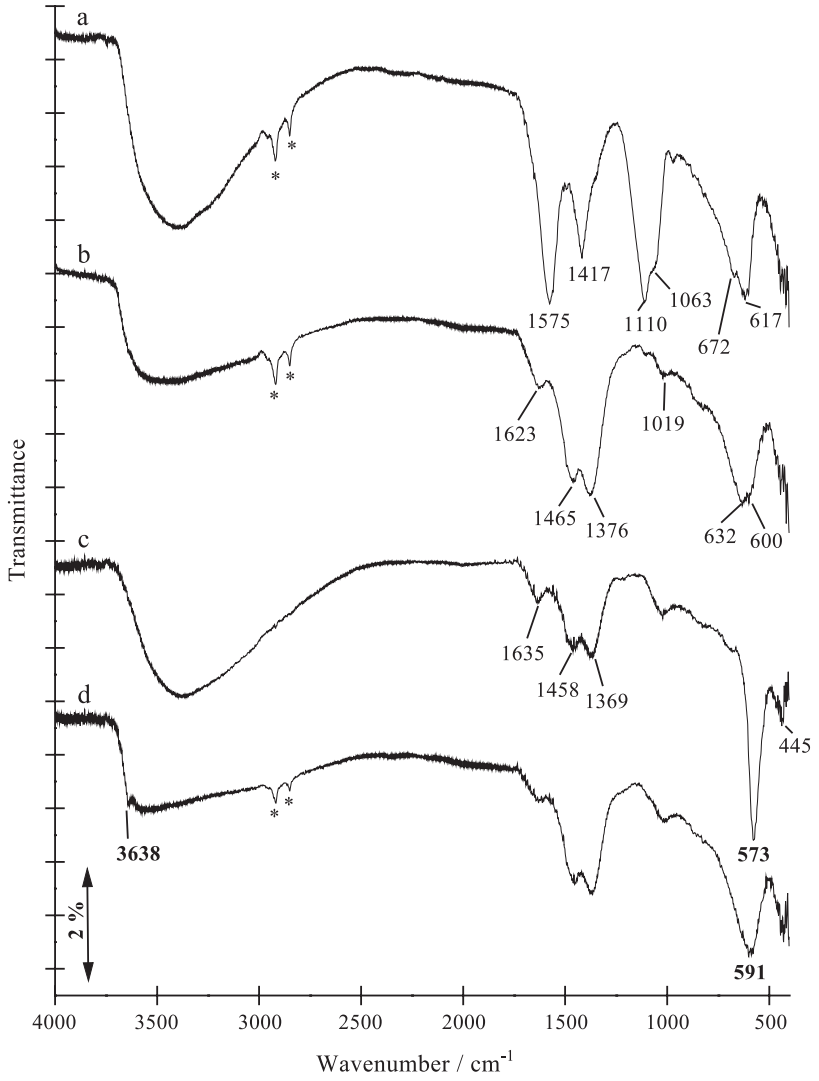

Fig. 7. Ex situ IR transmittance spectra of a thin film thermally treated at 270 °C for 15 min (a), after soaking for 5 min in 0.1 M LiOH (b), galvanostatically charged (c) and discharged (d), * denotes the absorbance of the glue deposited on copper tape. Copper tape is stick on the upper edge of Si resin to enable a better contact between Si and the external circuit.

diminished when the cycling proceeded because the formed hydrated secondary structure blurred the differences between the local structures of the Ni atoms in β(II) and β(III) phases.

4. Conclusion

The electrochromic response and electrochemical stability of the Ni-oxide films synthesised by the sol–gel route largely depended on the preparation conditions and the precursor used. We developed thermogravimetric technique, which allowed us to follow directly the decomposition of thin films deposited on glass substrates. Results showed that the temperature and decomposition rate of the formation of Ni-oxide differed with respect to the corresponding powders. TG technique applied on the films made possible to optimise the electrochromic response of the films by choosing the right heat treatment conditions in a

combination with different precursors (acetate, sulfate and nitrate). Ex situ IR spectroscopic studies of Ni-oxide films showed that the shift of the Ni–oxygen mode in charged/discharged film occurred. That we explained with the change of effective mass of –OH, $-OH_2$ groups vibrating with respect to the Ni atom which were not the same in β(II) and β(III) phase.

Acknowledgements

This work was supported by Grant PO-0508-0103 from the Ministry of Education, Science and Sport of the Republic of Slovenia.

References

[1] C.G. Granqvist, Handbook of Inorganic Electrochromic Materials, Elsevier, Amsterdam, 1995.
[2] K. Bange, T. Gambke, Adv. Mater. 2 (1990) 10.
[3] A. Šurca, B. Orel, B. Pihlar, J. Solid State Electrochem. 2 (1998) 38.
[4] R. Cerc Korošec, Dissertation, Ljubljana, 2001.
[5] A.M. Andersson, W. Estrada, C.G. Granqvist, A. Gorenstein, F. Decker, SPIE Proc. 1272 (1990) 96.
[6] K. Yoshimura, T. Miki, S. Tanemura, Jpn. J. Appl. Phys. 34 (1995) 2440.
[7] Z. Xuping, C. Guoping, Thin Solid Films 298 (1997) 53.
[8] T. Miki, K. Yoshimura, Y. Tai, M. Tazawa, P. Jin, S. Tanemura, The 3rd IUMRS International Conference on Advanced Materials, Tokyo, Japan, August 31–September 4, 1993, Article No. KP12.
[9] A. Šurca, B. Orel, B. Pihlar, P. Bukovec, J. Electroanal. Chem. 408 (1996) 83.
[10] X. Chen, X. Hu, J. Feng, Nanostruct. Mater. 6 (1995) 309.
[11] M. Chigane, M. Ishikawa, J. Electrochem. Soc. 14 (1994) 3439.
[12] R.M. Torresi, M.V. Vázquez, A. Gorenstein, S.I. Córdoba de Torresi, Thin Solid Films 229 (1993) 180.
[13] A. Gorenstein, F. Decker, M. Fantini, W. Estrada, SPIE Proc. 4 (1988) 272.
[14] C. Natarajan, H. Matsumoto, G. Nogami, J. Electrochem. Soc. 114 (1997) 121.
[15] W.W. Wendlandt, Thermal Methods of Analysis, Interscience Publishers, New York, 1964, p. 17.
[16] L. Niinistö, J. Therm. Anal. Calorim. 56 (1999) 7.
[17] M.C.A. Fantini, G.H. Bezerra, C.R.C. Carvalho, A. Gorenstein, SPIE Proc. 1536 (1991) 81.
[18] P.K. Sharma, M.C.A. Fantini, A. Gorenstein, Solid State Ionics 113–115 (1998) 457.
[19] A. Šurca, B. Orel, R. Cerc-Korošec, P. Bukovec, B. Pihlar, J. Electroanal. Chem. 433 (1997) 57.
[20] G. Boschloo, A. Hagfeldt, J. Phys. Chem., B 105 (2001) 3039.
[21] M. Leskelä, T. Leskelä, L. Niinistö, J. Therm. Anal. Calorim. 40 (1993) 1077.
[22] S. Lieb, R.K. MacCrone, J. Theimer, E.W. Maby, J. Mater. Res. 1 (1986) 792.
[23] J. Przyłuski, J. Płocharski, W. Bujwan, J. Therm. Anal. 21 (1981) 235.
[24] S. Hackwood, G. Beni, P.K. Gallagher, Solid State Ionics 2 (1981) 297.
[25] P.K. Gallagher, J. Therm. Anal. 38 (1992) 17.
[26] P.S. Gill, S.R. Sauerbrunn, B.S. Crowe, J. Therm. Anal. 38 (1992) 255.
[27] S. Benčič, B. Orel, A. Šurca, U. Lavrenčič Štangar, Sol. Energy 68 (2000) 499.
[28] K. Nakamoto, Infrared and Raman Spectra of Inorganic and Coordination Compounds, 5th ed., Wiley, New York, 1997, pp. 59–60, Part B.
[29] K. Nakamoto, Infrared and Raman Spectra of Inorganic and Coordination Compounds, 5th ed., Wiley, New York, 1997, pp. 80–81, Part B.
[30] C. Faure, C. Delmas, M. Fouassier, J. Power Sources 35 (1991) 279.
[31] K. Nakamoto, Infrared and Raman Spectra of Inorganic and Coordination Compounds, 5th ed., Wiley, New York, 1997, p. 86, Part B.
[32] P. Oliva, J. Leonardi, J.F. Laurent, C. Delmas, J.J. Braconnier, M. Figlarz, F. Filvet, J. Power Sources 8 (1982) 229.